DEVELOPMENTAL DYNAMICS 238:1974–1983, 2009

RESEARCH ARTICLE

Unified Description of Regeneration by Coupled Dynamical Systems Theory: Intercalary/Segmented Regeneration in Insect Legs

Hiroshi Yoshida[1]* and Kunihiko Kaneko[2]

Regeneration phenomena are ubiquitous in nature and are studied in a variety of experiments. *Positional information* and *feedback-loop hierarchy* are theories that have been proposed to explain ordering rules in regeneration; however, some regeneration phenomena violate the rules derived from them. In particular, grafted junction stumps with the same value/hierarchy sometimes lead to one extra segmented portion, termed *segmented regeneration*. To present a unified description of all insect leg regeneration phenomena, we propose a theoretical mechanism for regeneration without postulating positional information, by using a model that consists of intracellular reaction dynamics of chemical concentrations, cell-to-cell interactions, and an increase in cell number. As a normal developmental process, successive differentiation from pluripotent cells appears, as described by transition from cells with intracellular chaotic dynamics to those with oscillatory or fixed-point dynamics. By assigning chaotic and nonchaotic cell types to corresponding positions instead of positional information, intercalary, segmented, and tarsus regeneration are explained coherently. With this assignment of pluripotency to chaotic dynamics, a unified description of regeneration is obtained with some predictive value for new experiments. *Developmental Dynamics 238: 1974–1983, 2009.* © 2009 Wiley-Liss, Inc.

Key words: intercalary/segmented regeneration; isologous diversification theory; cell differentiation; coupled dynamical systems

Accepted 27 May 2009

INTRODUCTION

Development in multicellular organisms is a marvelous phenomenon consisting of several steps with a spatiotemporal order. Despite their complexity, they have robustness against perturbations. A demonstration of such robustness is seen in the regeneration of developed tissues. After macroscopic damage to tissues with the loss of some cells, the original spatial pattern of differentiated cell types is recovered. As a token of plasticity and robustness in development, regeneration phenomena have gathered interest from biologists over several decades (Hay, 1966; Meinhardt and Gierer, 1980; Forgács and Newman, 2005; Brockes and Kumar, 2008). To explain regeneration, *positional information* is often assumed. Positional information is defined as *instructions*, which are interpreted by cells to decide their differentiation with respect to their position relative to other parts. According to the positional information assumption, regeneration is explained as a process of cell division and differentiation so that noncontiguous *positional values* disappear through the increase in cell number (Gilbert, 2006). Indeed, several experimental results involving regeneration are well explained by this assumption of positional values: for instance, when nonadjacent por-

[1]Faculty of Mathematics, Kyushu University, Fukuoka, Japan
[2]Department of Pure and Applied Sciences, The University of Tokyo/Complex Systems Biology Project, ERATO, JST, Tokyo, Japan
***Correspondence to: Hiroshi Yoshida, Faculty of Mathematics, Kyushu University, Hakozaki 6-10-1, Higashi-ku, FUKUOKA 812-8581 Japan. E-mail: youshida.p@gmail.com**

DOI 10.1002/dvdy.22026
Published online 14 July 2009 in Wiley InterScience (www.interscience.wiley.com).

tions within a leg of the newt, crayfish, or cockroach are grafted together, localized cell division and differentiation occur to interpolate positional values of intermediate regions. This is known as intercalary regeneration (Bryant et al., 1977; Mittenthal and Trevarrow, 1983; Nakamura et al., 2008).

In this positional information theory, how positional information can be generated is not clear. In contrast, Hans Meinhardt proposed as one possible mechanism of positional information a chemical concentration gradient generated by a source at one end and a sink at the other end of the segment (Meinhardt and Gierer, 1980; Meinhardt, 1982). For the generation of positional information, he assumed chemical reactions consisting of two (or more) autocatalytic feedback loops, which suppress each other locally, but which activate each other by means of a diffusing substance. With this reaction and diffusion process, a chemical concentration pattern is generated without requiring external positional information to initiate the pattern (sequence). Intercalary regeneration is achieved by a hierarchy among the feedback loops, so that the original concentration pattern is restored.

However, some experiments are hard to explain by the positional information or Meinhardt's theory. When congruent grafting was performed between junction stumps (French, 1976), some of the graft/host junctions produced an extra portion. Although the adjacent cells take the same positional value, an extra portion of leg with a cell type that differs from that of the adjacent cells is generated. This process is termed *segmented regeneration*. According to the positional information, such differentiation of novel cell types between the same cell type cannot be explained.

To explain such a regeneration phenomenon, a dynamic process of differentiation from identical cell types is required. Indeed, one of the authors (K.K.) and Yomo proposed *isologous diversification* (Kaneko and Yomo, 1997, 1999; Furusawa and Kaneko, 1998, 2001) by considering interacting cells with intracellular reaction dynamics, where identical cells start to differentiate through cell division processes and cell-to-cell interactions. Based on this isologous diversification, the authors demonstrated that morphogenetic diversity and recursive production of patterns are compatible (Yoshida et al., 2005). Now, from this recursive production, regeneration of the original will be expected, while the diversity may allow for the generation of a novel part. Hence, it will be promising to apply the isologous diversification theory to the description of regeneration. In the present study, by using a simple model of interacting cells with coupled dynamics of a few chemicals, we demonstrate that this model can indeed explain both intercalary and segmented regeneration.

The present study is organized as follows. First, in Section 2, we survey regeneration experiments, with emphasis on regeneration of a cockroach's leg. Both the experiments obeying and violating the conventional models—the positional information and feedback-loop hierarchy—are described. In Section 3, we introduce a model for differentiation of cells aligned like a chain, by revising our earlier model (Yoshida et al., 2005) to adapt to the experimental situation. These cells have intracellular reaction dynamics of several chemicals, and they interact through such diffusing chemicals. Through successive cell divisions, the cells differentiate into five types to form an ordered pattern. In Section 4, we perform several types of numerical regeneration experiments adopting this model, and we find that both intercalary and segmented regeneration appear naturally. The mechanism for such regeneration is discussed in the Discussion section, to present a unified description.

SURVEY OF REGENERATION EXPERIMENTS

In this section, we briefly survey experiments on regeneration. Both intercalary and segment regeneration are described, and we show how positional information and feedback-loop hierarchies among cells explain the former type of regeneration but not the latter.

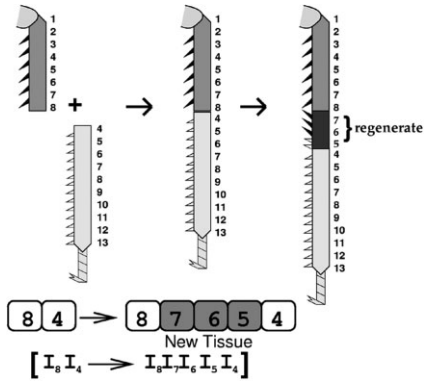

Fig. 1. The typical regeneration experiment of intercalary regeneration in the cockroach leg (Alberts et al., 2008). When mismatched portions of the growing legs are grafted together, new tissue is intercalated to fill in the gap so that the noncontiguous positional values disappear.

Experiments Obeying the Conventional Model

One of the clear experiments on regeneration was performed using the cockroach leg. In particular, the intercalary regeneration discovered in this model was a classic example of a description based on positional information values. Figure 1 depicts the regeneration experiment explained by positional values. Letters 1 to 13 denote physical levels of the leg segments corresponding to positional values 1 to 13. The figure shows the graft combination and its result after two moults. Intercalation occurs between noncontiguous positional values in the proximal–distal sequence when the grafts are between different tibiae. This regeneration is explained by the "shortest intercalation rule," which says that removal of a narrow, longitudinal strip of integument from any location results in stump healing, thereby confronting cells that are not normally adjacent. This leads to localized growth and intercalation. In subsequent larval stages, the leg regains its constituent cells with contiguous positional values by inserting the fewest possible cells. As illustrated in Figure 1, when normally nonadjacent cells 8 and 4 are put side by side, the gap will be filled by cells with the shortest possible sequence, 765, and not by a longer sequence such as 76545. The intercalary regeneration process is explained as a process that

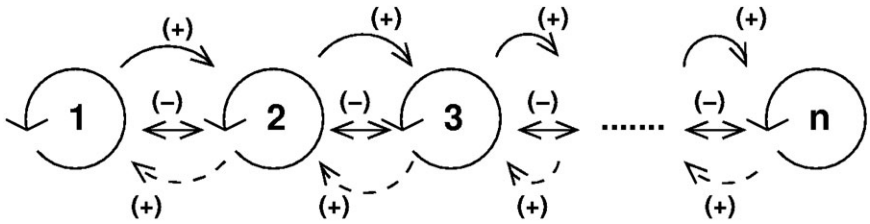

Fig. 2. Molecular interactions that enable the self-stabilizing structure (Meinhardt, 1982). Each state has a feedback loop on its own, denoting the autocatalytic gene activator. In addition, there is long range activation of its neighbors (−) and locally exclusive repression (−).

interpolates the information values with a minimal cell sequence.

In this theory, what the values of positional information 1,2,3,4,. . . specify are not answered. To overcome such criticism, Hans Meinhardt introduced a model of feedback-loop hierarchy among cells (Meinhardt and Gierer, 1980; Meinhardt, 1982), in which each cell state has a feedback loop of its own, caused by an autocatalytic process that activates gene expression. In addition, the expression is suppressed by an inhibitor with long-range coupling as illustrated in Figure 2. These activator–inhibitor dynamics are expressed by:

$$\begin{cases} \partial g_i/\partial t = c_i g_i^2/h - \alpha g_i \\ \qquad + D_{gi}\partial^2 g_i/\partial x^2, \\ \partial h/\partial t = \sum c_i g_i^2 - \beta h, \end{cases} \quad (1)$$

where g_i is the concentration of the ith activator, with an autocatalytic expression, with α and D_{gi} as its decay and diffusion constants, respectively, and h is the inhibitor synthesized through the activator and damped with the decay constant β. Distinct cell types are characterized by which of the g_i is expressed. As a hierarchy of the feedback loops, $c_i > c_{i+1}$ is assumed in Eq. [1]. Now, the operation of grafting amputated legs is given by putting adjacent cells with the expression of different g_i, say 4 and 8. At the mismatching junction, g_4 and g_8 molecules are exchanged between the cells. Then, according to the hierarchy $c_i > c_{i+1}$, g_4 dominates, leading to a decrease in the production of g_8 at the junction. If the expression of g_4 is sufficiently extended, then the expression of g_5 is induced between the two. In the same manner, g_6 is expressed between the cells expressing g_5 and g_8. By repeating such a process, the original sequence of 45678 is regenerated. Hence, intercalary regeneration is explained in terms of a hierarchy of feedback loops, $c_i > c_{i+1}$. This theory can explain what the values of positional information 1,2,3,4,. . . specify, whereas the validity of the hierarchy assumption (which is a bit demanding) still required examination.

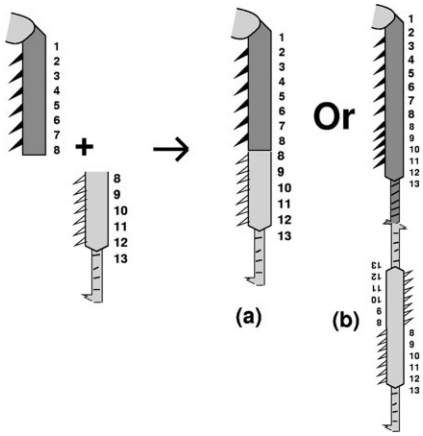

Fig. 3. a,b: Segmented regeneration: when the mid-tibia levels are grafted together, they sometimes lead to no segmented regeneration (a) or to segmented regeneration (b).

Segmented Regeneration and Number of Tarsomeres in Cockroach Legs

In addition to the intercalary experiment, there are also classic experiments on regeneration that, indeed, are hard to explain by "positional information" or "feedback-loop hierarchy."

One experiment concerns the combined series of congruent grafts made between mid tibiae (French, 1976). Figure 3 illustrates that the graft junction sometimes produces segmented structures. By following the conventional viewpoint, the junction is, of course, composed of cells with the same positional values or the same expressed gene in the feedback-loop hierarchy. However, this grafting produces an extra portion (segment) of leg. This formation of inhomogeneity from homogeneous positional values cannot be derived from the conventional models in which the regeneration results from noncontiguity of positional values or expressed genes at the junction.

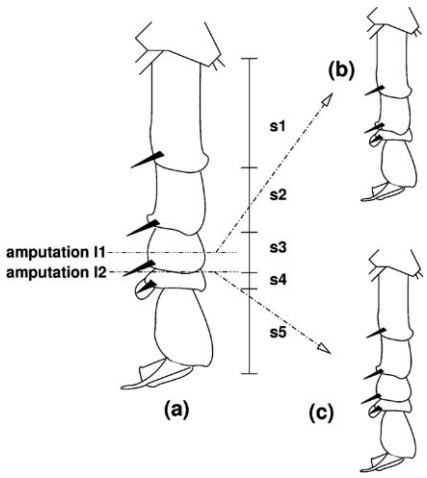

Fig. 4. Levels of amputation in the cockroach tarsus (Tanaka et al., 1992). **a:** Standard points of measurement in the adult. $s1$ to $s5$ denote the first to the fifth tarsomeres, respectively. **b:** When a tarsus is amputated at level $l1$ or more proximally, the regenerated tarsus tends to have four tarsomeres. **c:** By contrast, when a tarsus is amputated at level $l2$ or more distally, the regenerated tarsus tends to have five tarsomeres.

Another experiment is on the number of tarsomeres in the regenerated cockroach leg (tarsus) (Tanaka et al., 1992). There are five tarsomeres in the normal cockroach tarsus, as illustrated in Figure 4a, but the number of tarsomeres is often reduced in regenerated tarsi. Actually, when a tarsus is amputated at or proximal to the third tarsomere, only a four-segmented tarsus is regenerated (Fig. 4b), whereas when a tarsus is amputated distal to the third tarsomere, the regenerated tarsus has five segments (Fig. 4c). Some experiments on four-segmented regeneration also suggested that the missing tarsomere in regenerated tarsi corresponds to the third tarsomere of the normal five-segmented tarsus. To explain the disappearance of the third tarsomere in terms of positional values or feedback-loop hierarchy, the third tarsomere must have the same positional value as the second or the fourth tarsomere.

Developmental Dynamics

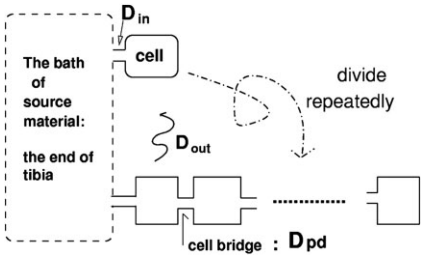

Fig. 5. Schematic representation of the model. The nutrient is supplied to the cell from the most proximal portion (end) of the tibia. Its concentration is X^0 at the most proximal portion. After a division, cells are interconnected, forming a cell bridge. By such cell divisions, cells are connected with one another as a one-dimensional chain.

However, a positional information or feedback-loop hierarchy model needs to assign distinct values of information for different positions by the assumption. Therefore, it is difficult to explain the above regeneration phenomenon.

In the present study, we adopt a model with isologous diversification. With this model, we explain both the intercalary and segmented regenerations, without any assumption of a hierarchy in gene expression levels.

MODEL: COUPLED CHAOTIC AND NONCHAOTIC CELLS

Before demonstrating regeneration of the cockroach leg, we first introduce our model, which outlines spontaneous cell differentiation and the generation of a spatial pattern. The model is represented schematically in Figure 5. In each cell, there are catalytic chemical reactions, including autocatalytic ones, which regulate the cell state and synthesize some chemicals for cell growth (membrane).

The concentration of the lst chemical inside the ith cell at time t is denoted by x_i^l. Here, a *nutrient chemical* "0" diffuses into cells from the most proximal portion of the tibia. The nutrient chemical merely means a representative chemical which exists outside the cells and diffuses into the cell. This chemical is not a catalyst but is necessary for growth in our model. The concentration of the nutrient is set to X^0 at the most proximal portion. At the i th cell, the concentration of the nutrient is assumed to be X^0/r_i, where r_i denotes the damping rate of $X^0$and depends only on the distance from the proximal end of leg. This nutrient diffuses into the cell with a diffusion coefficient D_{in}, while the corresponding concentration of the chemical within a cell is denoted by x_i^0. This nutrient is transformed successively to other chemicals through the catalytic reaction to produce other chemicals. These reaction dynamics are governed by a set of catalytic chemical reactions of Michaelis-Menten form as follows:

$$Met_i^l(t) = e\sum_{m,j} Con(m,l,j)\frac{x_i^l(t)\,x_i^m(t)}{1 + x_i^m(t)/x_M} - e\sum_{m,j} Con(l,m,j)\frac{x_i^l(t)\,x_i^j(t)}{1 + x_i^l(t)/x_M}, \quad (2)$$

where x_M is a parameter for the Michaelis-Menten form and e is the coefficient of the reaction. The reaction network is denoted by $Con(l,m,j)$, which is 1 when there is a path from chemical m to l catalyzed by chemical j, and 0 otherwise. It should be noted that $Con(m,0,0)$ is always 0 because the source material x_i^0 is not autocatalytic.

Now, $V_i(t)$ denotes the volume of the ith cell at time t. We assume that some chemicals produce the cell membrane materials, and that the chemicals decay linearly with a coefficient γ. This term is expressed as $\gamma P(l)x_i^l(t)$, where $P(l) = 1$ when x_i^l produces the membrane, otherwise $P(l) = 0$. To sum up, $V_i(t)$ grows as follows:

$$dV_i(t)/dt = V_i(t)k_m\gamma\sum_{l=1} P(l)x_i^l(t), \quad (3)$$

where k_m denotes the coefficient of the membrane material's contribution to the growth of $V_i(t)$. The ith cell divides into two when:

$$V_i(t) > 2V_0 \quad (4)$$

is satisfied, where V_0 is the initial volume. After the division, the daughter cell (numbered $i + 1$ here) has much the same concentration of chemicals as the mother cell i, i.e., x_i^l, and x_{i+1}^l, after a division, take $(1 + \varepsilon)x_i^l(t)$ and $(1 - \varepsilon)x_i^l$, respectively, where ε represents a small fluctuation caused by the cell division. In the present study, ε is taken as a random number over $[-10^{-4}, +10^{-4}]$, but this magnitude itself is not important for cell differentiation, provided it is not exactly zero. After a division, the two cells have the same volume, namely V_0. They remain connected with each other by forming a cell bridge (plasmodesma). Through this cell bridge, the chemicals of the two cells diffuse with the diffusion coefficient D_{pd}. After cell divisions, cells are interconnected to form a one-dimensional chain.

Only x_i^0 is supplied by a flow from the bath of source material X^0 with a normal diffusion coefficient D_{in}, while the other chemicals spread out slowly into the bath with a smaller diffusion coefficient D_{out}. This diffusion of each chemical is assumed to be proportional to the volume of the cell. Summing up all these processes, we have the following model equation:

$$dx_i^l(t)/dt = Met_i^l(t) + D_{\text{pd}}/V_i(t) \times \sum_{NN=\text{Nearest neighbour}} (x_{NN}^l(t) - x_i^l(t)) + \begin{cases} + D_{\text{in}}(X^0/r_i - x_i^0(t)) \\ \quad (l = 0) \quad [\text{the source material}] \\ - D_{\text{out}}x_i^l(t) - \gamma P(l)x_i^l(t) \\ \quad (l > 0) \quad [\text{the others}] \end{cases} - x_i^l(t)(dV_i(t)/dt)/V_i(t), \quad (5)$$

where r_i describes the damping rate of X^0. It may be worth noting that the employment of r_i is not essential to isologous diversification, indeed, it occurs without r_i (Yoshida et al., 2005).

Isologous Diversification: Dynamical Systems, Attractors, Chaos, and Multistability

In this subsection, we briefly explain the dynamical systems approach to cell differentiation, in particular *isologous diversification*. We first introduce notions of dynamical systems, attractors, and chaos. Then, we explain isologous diversification together with multistability.

A *dynamical system* is a mathematical description of the deterministic evolution of the state of a system (Hirsch et al., 2004). A typical example of a dynamical system is described by a system of ordinary differential equations:

$$\begin{cases} dx^1/dt = F_1(x^1,x^2,\ldots,x^n), \\ dx^2/dt = F_2(x^1,x^2,\ldots,x^n), \\ \vdots \\ dx^n/dt = F_n(x^1,x^2,\ldots,x^n), \end{cases}$$

where $F_i(1 \leq i \leq n)$ is a function of $x^1, x^2,\ldots,x^n$.

The space $(x^1, x^2,\ldots, x^n)$ is referred to as the *phase space*. For example, it can represent a set of concentrations of chemicals within a cell. The path in phase space is referred to as the *orbit* or *trajectory*. An *attractor* is a bounded set to which regions of initial conditions asymptote as a dynamical system evolves. An attractor can be a fixed-point, a periodic, or a quasi-periodic motion. However, there is also a *chaotic attractor* that is neither periodic nor describable as a combination of several periodic motions. *Chaos* is an attractor with irregular oscillation, where small differences in initial conditions are amplified exponentially, even though it has asymptotic stability as an attractor. (See also the Appendix of Furusawa and Kaneko, 2001).

The notion of *isologous diversification* was proposed by Kaneko and Yomo (1997, 1999) to simulate stable cell differentiation against molecular and other fluctuations. Consider a cell with internal dynamical systems (in terms of gene expression levels) and cell-to-cell interactions. The cells that have divided from a single cell have the same dynamics of chemicals, so that they maintain synchronization of oscillation of their intracellular state up to cell number. However, such homogeneity among cells becomes destabilized as the number increases. Any small difference between cells caused by noise or by cell division is amplified, so that the phase of synchrony of oscillations is lost. With further increases in numbers, the cells start to take different chemical compositions, which are stable attracting states. A few attracting cellular states appear, maintained by intracellular dynamics and cell-to-cell interactions. In other words, the interaction between the states maintains their stability: this is the phenomenon of *multistability*.

The theory of such "spontaneous cell differentiation" was pioneered by Alan Turing, who showed that a reaction–diffusion system can produce an inhomogeneous, stable pattern (Turing, 1952). Independently of initial conditions, concentrations of chemicals can form a stripe or wave pattern, and this pattern formation has robustness against perturbations. However, neither sufficiently complex intracellular dynamics nor *an increase in cell number* was introduced. As mentioned above, by taking account of intracellular dynamics, together with an increase in cell number, *isologous diversification* was proposed (Kaneko and Yomo, 1997, 1999). An important difference between Turing's model and that of isologous diversification lies in the interpretation of cell types. In the latter, different cell types belong to different attracting states in the phase space. By contrast, in the Turing model, different types correspond to mere different phases in the wave either in space or in time. Furthermore, in isologous diversification, cells with chaotic dynamics are shown to function as stem cells, as slight difference in concentrations within a cell is amplified, leading to a differentiated cell type (Furusawa and Kaneko, 1998, 2001). Thus, by extending the system to include spatial interaction, positional information is generated spontaneously (Furusawa and Kaneko, 2000), and this is essential to the capacity for regeneration.

RESULTS

We have performed simulation experiments for a variety of randomly chosen reaction networks: *Con* of Eq. [2] and parameters in the Eq. [3] and [5]. For some networks, the reaction dynamics fall onto fixed points, and cells do not differentiate, and simple homogeneous patterns are formed. For some other networks, however, cells differentiate into several types, which have distinct chemical compositions as the cell number increases. In this case, chemical concentrations of the initial cell type show irregular oscillatory dynamics as known as chaos. By cell division, another cell type appears, from which another cell type differentiates later. In this study, we adopt networks that exhibit such cell differentiation, to examine the possibility of regeneration. To be specific, we adopt the same network topology as used in (Yoshida et al., 2005), where the network consists of 20 chemical species with four autocatalytic and three nonautocatalytic paths from each, on average. For detailed of the adopted network, see Appendix A. We examine 180 randomly generated networks, 22% of which exhibit fixed-point behavior, 30% exhibit (quasi)periodic behavior, 37% and 11% exhibit chaotic and isologous diversification behaviors, respectively.

Furthermore, we investigate also catalytic chemical reactions of Hill form: $xy^n/(1 + y^n/x_M)$ corresponding to the existence of cooperative behavior of chemicals.

Among randomly generated 143 samples of $n = 2$, 83% exhibit fixed-point behavior, 14% exhibit (quasi)periodic behavior, 2.1% and 1.4% exhibit chaotic and isologous diversification behaviors, respectively. Likewise, among randomly generated 190 samples of $n = 3$, 94% exhibit fixed-point behavior, 4.2% exhibit (quasi)periodic behavior, 1.1% and 0.53% exhibit chaotic and isologous diversification behaviors, respectively. As long as we use a network that allows for isologous diversification behaviors, the regeneration process to be discussed is as follows. Note also that the fraction of networks showing oscillatory dynamics is not major, but they are selected through evolution as they have higher growth speed as an ensemble of cells (Furusawa and Kaneko, 2000).

First, we describe differentiation starting from a single cell, without any external operation. Here, five cell types appear successively, as shown in the cell lineage diagram in Figure 6a, where each cell type T_1,T_2,T_3,T_4 and T_5 (in order of appearance) is represented by a color: red, green, blue, magenta, and cyan, respectively. The differentiation from T_1 to T_2, then from T_2 to T_3, from T_3 to T_4, from T_4 to T_5 occurs successively, i.e., with the cell lineage $T_1 \Rightarrow T_2 \Rightarrow T_3 \Rightarrow T_4 \Rightarrow T_5$. Each cell type has a distinct chemical composition of 20 chemical species. The orbit is plotted for two chemical components in Figure 7a, while the time course of concentrations for T_1, T_2, and T_3 cells is plotted in Figure 7b. The temporal variation is decreased as the differentiation from T_1 progresses. The attractors of each cell type are chaotic (T_1), quasi-periodic (T_2), periodic (T_3), periodic (T_4), and fixed point (T_5), respectively. As a spa-

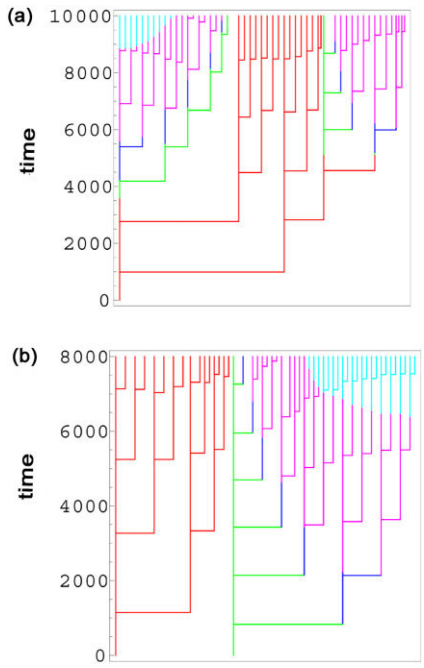

Fig. 6. The cell lineage diagram. **a:** When started from a single chaotic (red) cell (T_1), a pattern of cell types is formed on the initial condition of chaotic intracellular dynamics. The parameters are $X^0 = 1.5, r_i = (1 + 0.01d_i$ $e = 0.3, x_M = 5.0, k_m = 0.1, \gamma = 10^{-3}, V_0 = 5.0, D_{\text{in}} = 0.01, D_{\text{pd}} = 0.1$, and $D_{\text{out}} = 10^{-4}$, where d_i denotes the distance from the proximal end of leg. **b:** A cell lineage diagram started from T_1T_2. In this case, two initial cells, a chaotic attractor (red, T_1) and a quasi-periodic *partial* attractor (green, T_2) are grafted together. Even when starting from T_1 and T_3, T_4, or T_5, the same pattern ($T_1T_2T_3T_4^{n_4}T_5^{n_5}$,$n_4$,$n_5 > 1$) eventually appears within the cell chain thus produced.

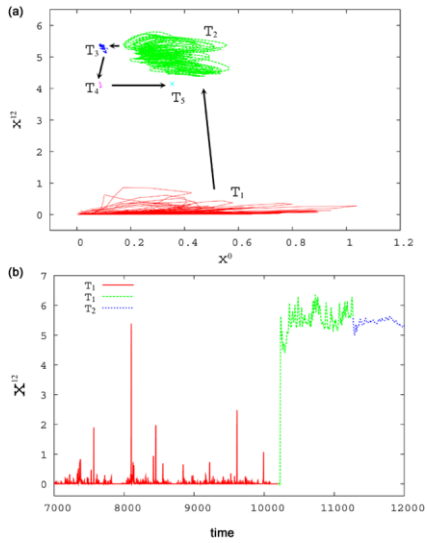

Fig. 7. Dynamics of the cell lineage diagram. **a:** The orbits of chemical concentrations are plotted using (x^0,x^{12}). The five colors (red, green, blue, magenta, and cyan) denote a chaotic attractor (T_1), a quasi-periodic *partial* attractor (T_2), a periodic *partial* attractor (T_3), a periodic *partial* attractor (T_4), and a fixed point (T_5), respectively. The transition between the dynamics is $T_1 \Rightarrow T_2 \Rightarrow T_3 \Rightarrow T_4 \Rightarrow T_5$. **b:** Temporal change of concentrations of cell types T_1, T_2, and T_3, using the chemical x^{12}.

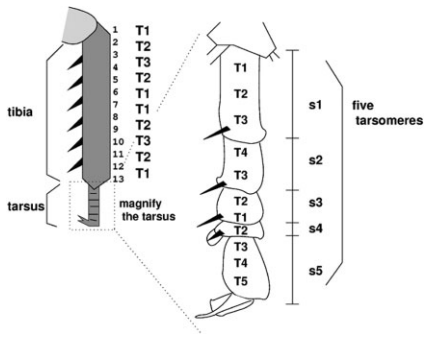

Fig. 8. Assignment of chaotic cell type T_1 and nonchaotic type $T_2,\ldots,T_5$ to the cockroach legs. We propose the assignment as illustrated by the figure. There is a difference between our proposed assignment and the positional information. In the positional information or feedback-loop hierarchy models, the mid-tibia level corresponds to the "middle" of the values or the hierarchy denoted by 6 to 8. In contrast, in our model, the mid-tibia level corresponds to the chaotic cell-type T_1. Likewise, the distal portion of the third tarsomere level $s3$ corresponds to T_1.

tial pattern, these cell types are aligned in the order of these types, so that the pattern sequence $T_1^{n1}T_2^{n2}T_3^{n3}T_4^{n4}T_5^{n5}(n_i \geq 1,1 \leq i \leq 5)$ is generated.

Simulations of Intercalary Regeneration

Next, using the above model with the cell lineage diagram (Fig. 6a), we performed a "numerical regeneration experiment." We observed the ability for regeneration. By starting from any adjacent pair of cell types such as $T_1 + T_2$, $T_1 + T_3$, $T_1 + T_4$, and $T_1 + T_5$, the pattern generated by "normal development": $T_1^{n1}T_2^{n2}T_3^{n3}T_4^{n4}T_5^{n5}$ $(n_i \geq 1,1 \leq i \leq 5)$ is always generated (See Fig. 6b) ($T_1 + T_2$ case). This result can be interpreted as the regeneration of a cell-chain pattern composed of contiguous types: T_1,T_2,T_3,T_4 and T_5. Generally speaking, the intermediate cell types $T_iT_{i+1}\ldots T_j$ $(1 < i \leq j < n)$ are regenerated from the graft junction $T_{i-1} + T_{j+1}$ under the cell lineage diagram $T_1 \Rightarrow T_2 \Rightarrow \ldots \Rightarrow T_i \Rightarrow \ldots \Rightarrow T_j \Rightarrow \ldots T_n$.

This result is interpreted as intercalary regeneration. In the experiment on the cockroach leg, the regeneration arises by putting together two parts with noncontiguous positional values. Here, we can match the ordering of cell type T_i with $i = 1,2,3,\ldots$ to this positional value or to the type of gene in the hierarchy in the feedback-loop model, as illustrated in Figure 8. The intercalary regeneration is a natural consequence of the ordering of T_i, as the intracellular dynamics and cell-to-cell interaction support the appearance of only the sequence of continuous change of i in T_i. Note also that we do not need any assumption of hierarchy in our model. The ordering of T_i emerges as a natural consequence of intra- and intercellular coupled dynamics, leading to successive decrease in temporal variation, as given in Figure 7.

Simulations of Segmented and Tarsus Regenerations

Next, we performed two other sets of numerical regeneration experiments that corresponded to "segmented regeneration" and "tarsus regeneration" experiments, using the same model. In the segmented regeneration, the graft junction, T_iT_i, sometimes produces an extra portion with different cell types $T_j(i \neq j)$, while in the tarsus regeneration, the distinct tarsomeres must correspond to the same value as mentioned in Section 2. These two regenerations are puzzling, because in conventional models, nothing is expected to occur from the same-value junction T_iT_i, and the distinct portions are assigned to distinct values.

To simulate segmented regeneration, both ends of the junction have to be of the same cell type, assumed to be T_1, a chaotic cell type. To set up the configuration illustrated in Figure 8, there is freedom in the assignment of other cells. For instance, we assign $T_1,T_2,T_3,\ T_2,T_1,T_1,\ T_2,T_3,T_2,T_1$ to the positional-value portions 1 to 13, respectively. Likewise, to consider tarsus regeneration, we assume that at one end there is a T_1 cell type. Here again, there is freedom in the assignment of other types, but as an instance, we assign $T_1,T_2,T_3,\ T_4,\ T_3,\ T_2,\ T_1,\ T_2,\ T_3,\ T_4,T_5$ to the tarsomeres. In

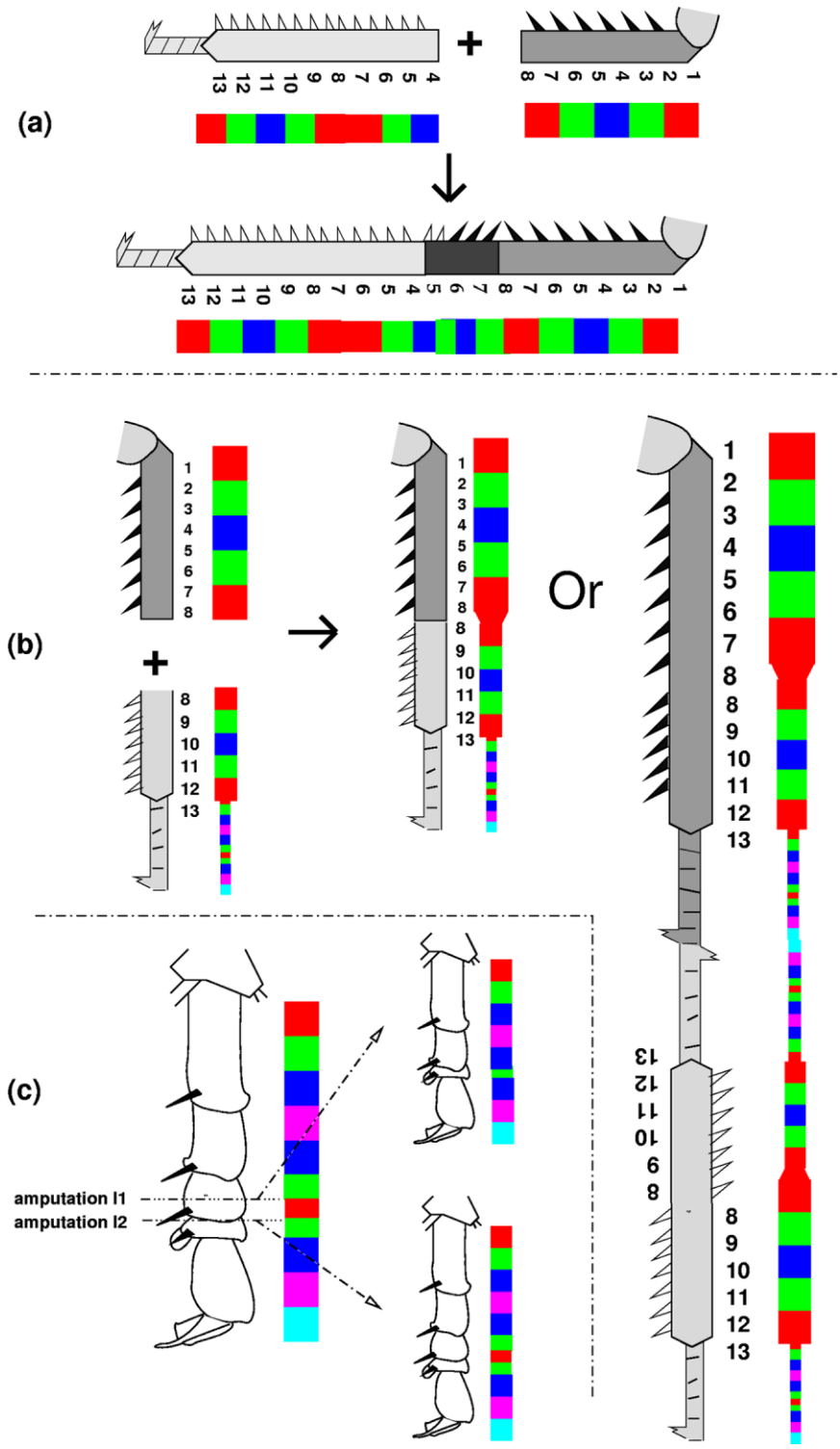

Fig. 9. The correspondence between the intercalary/segmented/tarsus regeneration and our simulation experiment. **a:** Intercalary regeneration and our cell type assignments. **b:** Segmented regeneration. **c:** Tarsus regeneration.

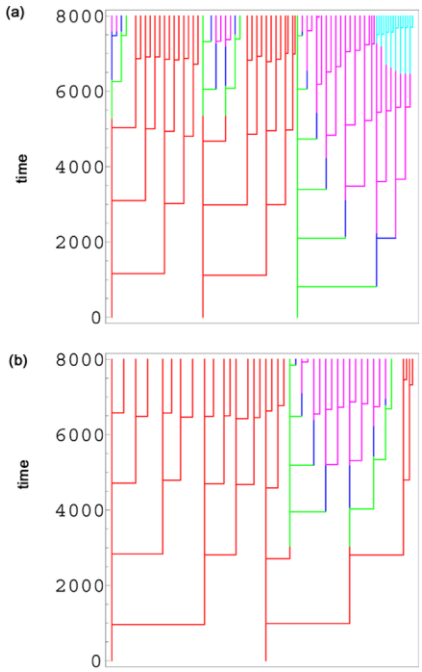

Fig. 10. Simulation experiments for segmented regeneration. **a:** When starting with $T_1T_1T_2$, one segment $T_1T_2T_3T_4^4T_3T_2T_1$ eventually appears in the cell chain. **b:** The pattern when starting with T_1T_1.

contrast to the conventional model, the most distal end of the tibia is assigned to T_1, the chaotic cell type, the same type as in the most proximal portion.

Note that the essence here is the use of the T_1 cell type, i.e., the assignment of both ends and the center of the tibia to a chaotic cell type T_1 for segmented regeneration, and the assignment of the distal portion of the third tarsomere (s_3, in the figure) to T_1 for tarsus regeneration. The results to be discussed below are also obtained as long as the interval cell types between two T_1 s are $T_2T_3\ldots T_{j-1}T_jT_{j-1}\ldots T_2 (n \geq j \geq 2)$ under the cell-lineage diagram $T_1 \Rightarrow T_2 \Rightarrow \ldots \Rightarrow T_i \Rightarrow \ldots \Rightarrow T_j \Rightarrow \ldots \Rightarrow T_n$. In fact, the assignment to T_1 is in part supported by the observation that X-irradiation of this terminal zone blocks the regeneration of an amputated tarsus (Bullière and Bullière, 1985, Ch. 2.3.1, Fig. 13a), i.e., without the cell type corresponding to T_1, regeneration does not occur, as is also supported by the simulation below.

Figure 10a shows the cell chain pattern produced when simulations are started with $T_1T_1T_2$ for segmented regeneration. In contrast to Figure 6b (starting with T_1T_2), segment $T_1T_2T_3T_4^4T_3T_2T_1$ sometimes arises from T_1T_1 within the produced cell chain. In fact, five and nine among 30 trials have exhibited segmentation up to time 8000 when starting from T_1T_2 and $T_1T_1T_2$, respectively. (French [1976] reported that actual segmented regeneration occurred at a probability of 9/278

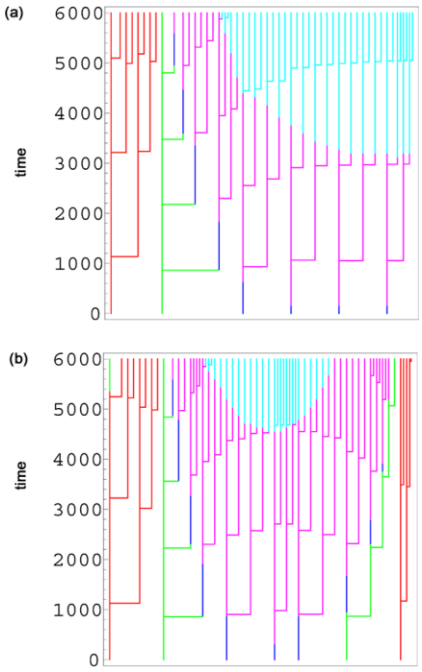

Fig. 11. Simulation experiments for tarsus regeneration. **a:** When starting with $T_1T_2T_3T_4T_3T_2$, namely amputation level $l1$ in Figure 4, the pattern $T_1^4T_2T_3T_4^6T_5^{n_5}$, $n_5 > 1$ appears at time around 4000. **b:** When starting with $T_1T_2T_3T_4T_3T_2T_1$, namely amputation level $l2$, $T_1^4T_2T_3T_4^{n_4}T_3T_2T_1^4$, $n_4 > 1$ appears at time around 4000.

from the graft junction.) This indicates that grafting of a T_1 into a T_1 cell can produce the segment: in other words, segmented regeneration, at a certain probability, occurs from a graft junction between mid tibiae having the same cell type T_1, the chaotic cell type. The correspondence between segmented regeneration and our model is given in Figure 9b.

Last, to simulate the other regeneration phenomenon, tarsus regeneration, we started with $T_1T_2T_3T_4T_3T_2$ and $T_1T_2T_3T_4T_3T_2T_1$, which correspond to amputations proximal and distal to the third tarsomere, respectively. The produced cell-chain patterns are illustrated in Figure 11a,b. The former, corresponding to amputation level $l1$ in Figure 4, produces a pattern $T_1^4T_2T_3T_4^6T_5^{n5}$,$n_5 > 1$, while the latter, corresponding to amputation level $l2$, produces a pattern $T_1^4T_2T_3T_4^{n4}T_3T_2T_1^4$,$n_4 > 1$ at time around 4000. In view of the composition of cell types of these two patterns, these two regenerations correspond to four-segmented and five-segmented tarsi (Figs. 4b,c), respectively. The correspondence between segmented regeneration and our model is given in Figure 9c.

DISCUSSION

By using a simple model with inter–intra reaction dynamics, we have succeeded in reproducing regeneration experiments in cockroach legs, with which we can explain coherently those regeneration phenomena both obeying and violating the conventional models.

Now, let us examine differences between the two conventional models and ours. In the former models, regeneration is explained as recovery from noncontiguous values of positional information, or a feedback-loop hierarchy. Therefore, these models are hard to explain segmented regeneration, wherein noncontiguous values/hierarchies do not exist. By contrast, in our model starting with T_1T_1 cell types, with an increase in cell number, spontaneous changes in cell types arise by means of internal chaotic reaction dynamics. In our model, although we have not postulated different values or hierarchies depending on cell positions in advance, intracellular chemical reaction dynamics that can be chaotic produce cell types spontaneously.

Based on this isologous diversification, in our previous study (Yoshida et al., 2005), we searched for conditions compatible with cell type diversity and recursive production. In the present model, recursive production has been achieved by combining a chaotic cell (T_1) and a nonchaotic cell (T_i,$i \geq 2$), while morphogenetic diversity arises mainly from chaotic dynamics T_1. Therefore, the balance between T_1 and $T_i(i \geq 2)$ plays an important role in a compatible condition.

Now, let us scrutinize segmented regeneration from the perspective of our model. As illustrated in Figure 3, even a graft junction between cells of the same type produces segmented structures at a certain level of probability. For better understanding, we performed a simulation experiment starting with T_1T_1, as illustrated in Figure 10b. T_1T_1 often produces the segmented pattern $T_1T_2T_3T_4^{n4}T_3T_2T_1$,$n_4 > 1$. The probability of production of this pattern was found to be higher than that when we started with T_1 only. This observation suggests that segmented regeneration arises from contiguous chaotic cells. Note that chaotic dynamics produce stochastic behavior, which explains the probabilistic occurrence of segmented regeneration observed experimentally. Such a probabilistic occurrence of tarsus regeneration is also explained by assuming the existence of T_1 cell types producing chaotic dynamics.

There has been no direct experimental demonstration of chaotic oscillation, but two recent experiments suggest the existence of oscillatory and itinerant gene expression dynamics in stem cells. First, Shimojo et al. (2008) reported the existence of oscillations in gene expression in neural stem cells. The importance of oscillatory dynamics in somitogenesis is now established (Palmeirim et al., 1997), while such oscillation might also exist in short-germ or intermediate band stripe formation in insects (Fujimoto et al., 2008). Second, slow transitory dynamics in gene expression levels in stem cells have also been reported recently (Chang et al., 2008).

Summing up, we propose a unified description of regeneration phenomena: those obeying the conventional models correspond to the cell chain starting with $T_1T_i(i \geq 2)$, while those violating conventional explanations correspond to the cell chain starting with T_1T_1. It should be noted that to date we have not found leg regeneration experiments violating our model.

Prediction

Here, we have proposed an assignment that both the ends and the middle of the tibia correspond to the chaotic cell type T_1. In contrast, under positional information or feedback-loop hierarchy assumptions, the tibia is assigned to contiguous numbers in an ascending order (in the figures, numbers 1 to 13). Based on this definite difference, one can make an experimental prediction as follows. If one performs a regeneration experiment so that the middle level of the tibia is removed, the regenerated tibia will become shorter. This happens in almost the same manner as the missing tarsomere in the tarsus regenera-

tion experiment addressed in the Survey of Regeneration Experiments section. Generally, it is predicted that a regeneration experiment including a chaotic cell (T_1) performs segmented regeneration with a certain probability, whereas experiments consisting only of nonchaotic cells produce "shortened" regeneration.

Recently, cricket leg regeneration was investigated using RNA interference based on Meinhardt's model (Nakamura et al., 2008). Therefore, the cricket's leg can be a promising candidate to test our theory. Furthermore, with current visualization techniques, it will be possible to test our chaos hypothesis. Indeed, as with gene expression in stem cells, such experiments are ongoing (Chang et al., 2008; Shimojo et al., 2008). According to our study, pluripotent cells exhibit chaotic gene expression dynamics. If such cells with chaotic dynamics can grow and divide, proliferation or differentiation of other cell types will progress from them. Considering the capacity for regeneration in the insect leg, it is natural to expect the proliferation of pluripotent cells, so that division of chaotic cells will be expected, at least under some condition.

SUMMARY

In the present study, we have modeled regeneration phenomena in the cockroach leg by using cell chains with chaotic and nonchaotic dynamics. This model allows spontaneous cell differentiation through cell-to-cell interactions. Morphogenetic diversity arises from chaotic dynamics, while regeneration arises from a balance between chaotic and nonchaotic cells. From this viewpoint, segmented regeneration is regarded as a result of imbalance between these distinct cells or perturbation toward chaotic cells. We have proposed a unified description: intercalary and segmented regeneration phenomena correspond to balance and imbalance between chaotic and nonchaotic cells, respectively.

ACKNOWLEDGMENTS

We thank Prof. Sumihare Noji and Dr. Taro Mito for valuable discussions on insect legs. This study was supported in part by the Program for Improvement of the Research Environment for Young Researchers from the Special Coordination Funds for Promoting Science and Technology (SCF), commissioned by the Japan Science and Technology Agency (JST).

REFERENCES

Alberts B, Johnson A, Lewis J, Raff M, Roberts K, Walter P. 2008. Molecular biology of the cell. 5th ed. New York: Garland Science.

Brockes JP, Kumar A. 2008. Comparative aspects of animal regeneration. Annu Rev Cell Dev Biol 24:525–549.

Bryant PJ, Bryant SV, French V. 1977. Biological regeneration and pattern formation. Sci Am 237:67–81.

Bullière D, Bullière F. 1985. Regeneration. In: Postembryonic development. Oxford: Pergamon Press. p 371–424.

Chang HH, Hemberg M, Barahona M, Ingber DE, Huang S. 2008. Transcriptome-wide noise controls lineage choice in mammalian progenitor cells. Nature 453:544–547.

Forgács G, Newman S. 2005. Biological physics of the developing embryo Cambridge, UK: Cambridge University Press.

French V. 1976. Leg regeneration in the cockroach, Blattella germanica I. Regeneration from a congruent tibial graft/host junction. Roux Arch Dev Biol 179:57–76.

Fujimoto K, Ishihara S, Kaneko K. 2008. Network evolution of body plans. PLoS ONE 3:e2772.

Furusawa C, Kaneko K. 1998. Emergence of rules in cell society: differentiation, hierarchy, and stability. Bull Math Biol 60:659–687.

Furusawa C, Kaneko K. 2000. Origin of complexity in multicellular organisms. Phys Rev Lett 84:6130–6133.

Furusawa C, Kaneko K. 2001. Theory of robustness of irreversible differentiation in a stem cell system: chaos hypothesis. J Theor Biol 209:395–416.

Gilbert SF. 2006. Developmental biology. 8th ed. Sunderland, MA: Sinauer Associates, Inc. 817 p.

Hay ED. 1966. Regeneration. New York: Holt, Rinehart and Winston.

Hirsch M, Smale S, Devaney RL. 2004. Differential equations, dynamical systems, and an introduction to chaos. Amsterdam: Elsevier Academic Press.

Kaneko K, Yomo T. 1997. Isologous diversification: a theory of cell differentiation. Bull Math Biol 59:139–196.

Kaneko K, Yomo T. 1999. Isologous diversification for robust development of cell society. J Theor Biol 199:243–256.

Meinhardt H. 1982. Models of biological pattern formation. London: Academic Press.

Meinhardt H, Gierer A. 1980. Generation and regeneration of sequence of structures during morphogenesis. J Theor Biol 85:429–450.

Mittenthal JE, Trevarrow WW. 1983. Intercalary regeneration in legs of crayfish: central segments. J Exp Zool 225:15–31.

Nakamura T, Mito T, Bando T, Ohuchi H, Noji S. 2008. Molecular and cellular basis of regeneration and tissue repair: dissecting insect leg regeneration through RNA interference. Cell Mol Life Sci 65: 64–72.

Palmeirim I, Henrique D, Ish-Horowicz D, Pourquié O. 1997. Avian hairy gene expression identifies a molecular clock linked to vertebrate segmentation and somitogenesis. Cell 91:639–648.

Shimojo H, Ohtsuka T, Kageyama R. 2008. Oscillations in Notch signaling regulate maintenance of neural progenitors. Neuron 58:52–64.

Tanaka A, Akahane H, Ban Y. 1992. The problem of the number of tarsomeres in the regenerated cockroach leg. J Exp Zool 262:61–70.

Turing AM. 1952. The chemical basis of morphogenesis. Philos Trans R Soc B 237:37–72.

Yoshida H, Furusawa C, Kaneko K. 2005. Selection of initial conditions for recursive production of multicellular organisms. J Theor Biol 233:501–514.

APPENDIX A: PARAMETERS AND NETWORK STRUCTURE

Here, we show the parameters and network structure to exhibit isologous diversification and regeneration phenomena, as mentioned in the Results section.

The parameters are $X^0 = 1.5$, $r_i = (1 + 0.01d_i)$, $e = 0.3$, $x_M = 5.0$, $k_m = 0.1$, $\gamma = 10^{-3}$, $V_0 = 5.0$, $D_{\text{in}} = 0.01$, $D_{\text{pd}} = 0.1$, and $D_{\text{out}} = 10^{-4}$, where d_i denotes the distance from the proximal end of the leg. The network structure is described as the values of $Con(m,l,j)$. The pairs of (m,l,j) where $Con(m,l,j)$ is 1 are the following: (m,l,j) = (2,1,5),(0,4,11),(0,4,18),(0,8,7), (0,12, 1), (0,13,16),(0,15,7),(0,17,2),(0,19,9), (1,4,4),(1,5,5),(1,6,6),(1,8,15),(1,16, 16),(1,17,9),(2,0,1),(2,0,3),(2,4,17),(2, 5,5),(2,7,7),(2,9,9),(3,2,18),(3,12,12), (3,13,13),(3,14,14),(3,14,19),(3,15,4), (4,0,8),(4,2,15),(4,6,6),(4,11,11),(4,12, 12),(4,15,18),(4,16,16),(5,11,11),(5,12, 12),(5,13,14),(5,13,15),(5,15,15),(5,18, 17),(5,18,18),(6,4,1),(6,8,8),(6,8,17),(6, 9,16),(6,10,10),(6,15,15),(6,17,17),(7,1, 5),(7,5,12),(7,6,6),(7,8,8),(7,12,12),(7, 18,4),(8,3,3),(8,5,5),(8,10,10),(8,11,3), (8,11,11),(8,12,10),(8,16,18),(9,5,5),(9, 8,8),(9,13,10),(9,14,14),(9,17,19),(9,18, 18),(10,0,3),(10,3,16),(10,6,6),(10,7,3), (10,13,13),(10,14,14),(10,15,15),(11,1, 1),(11,3,5),(11,6,6),(11,12,12),(11,15,

18),(11,16,16),(12,0,11),(12,3,19),(12,4,4),(12,7,7),(12,9,9),(12,15,11),(13,3,3),(13,10,4),(13,16,4),(13,17,17),(13,18,4),(13,19,19),(14,6,6),(14,11,11),(14,11,16),(14,15,15),(14,16,16),(15,2,2),(15,4,1),(15,6,8),(15,14,14),(15,16,16),(15,18,4),(15,18,18),(16,3,17),(16,9,1),(16,9,9),(16,10,10),(16,17,11),(16,17,17),(16,18,18),(17,1,6),(17,2,2),(17,5,5),(17,7,6),(17,8,8),(17,10,10),(17,19,1),(18,2,2),(18,9,9),(18,9,13),(18,10,10),(18,12,16),(18,13,8),(19,1,1),(19,2,6),(19,6,14),(19,12,12),(19,16,16), where $l = j$ denotes an autocatalytic reaction path.

The membrane-producing chemicals are x^4,x^5,x^{11},x^{12}, and x^{16}.

We show another network structure exhibiting regeneration, where $X^0 = 1.5$, $r_i = (1 + 0.001d_i)$ $e = 0.3$, $x_M = 5.0$, $k_m = 0.1$, $\gamma = 10^{-3}$, $V_0 = 5.0$, $D_{\text{in}} = 0.01$, $D_{\text{pd}} = 0.01$, and $D_{\text{out}} = 10^{-4}$. The pairs of (m,l,j) where $Con(m,l,j)$ is 1 are: (m,l,j) = (0,2,6),(0,2,19),(0,4,6),(0,7,9),(0,10,18),(0,13,6),(0,14,8),(0,17,4),(0,17,14),(0,18,18),(1,2,2),(1,4,4),(1,4,12),(1,12,9),(1,16,9),(1,18,18),(2,6,6),(2,8,8),(2,8,9),(2,13,15),(2,15,15),(2,18,18),(3,4,4),(3,5,5),(3,5,15),(3,10,10),(3,11,7),(3,17,17),(4,3,9),(4,13,13),(4,14,15),(4,15,15),(4,17,17),(4,19,12),(5,1,1),(5,1,13),(5,3,15),(5,6,6),(5,8,15),(5,10,10),(5,13,13),(6,1,1),(6,4,4),(6,5,5),(6,9,16),(6,10,11),(6,14,12),(6,18,18),(7,0,4),(7,6,3),(7,9,9),(7,11,11),(7,11,19),(7,16,16),(7,17,17),(8,4,4),(8,6,14),(8,7,4),(8,7,7),(8,7,11),(8,9,9),(8,11,11),(9,1,1),(9,6,5),(9,6,6),(9,7,7),(9,11,11),(9,18,16),(10,0,9),(10,2,2),(10,4,4),(10,5,5),(10,12,18),(10,14,17),(10,16,16),(11,4,18),(11,8,8),(11,12,7),(11,13,12),(11,13,13),(11,19,19),(12,0,7),(12,2,8),(12,6,6),(12,11,11),(12,17,8),(12,18,18),(13,1,1),(13,3,3),(13,4,9),(13,5,11),(13,6,18),(13,12,12),(14,1,11),(14,3,3),(14,9,18),(14,10,10),(14,11,12),(14,13,13),(14,15,15),(15,1,1),(15,2,4),(15,8,8),(15,11,4),(15,11,14),(15,12,12),(15,14,14),(16,2,2),(16,6,6),(16,7,7),(16,10,3),(16,13,14),(16,14,18),(17,19,19),(18,1,1),(18,3,12),(18,13,13),(18,13,19),(19,1,1),(19,1,10),(19,5,1),(19,7,7),(19,11,11),(19,12,10). In this case, the membrane-producing chemicals are x^5, x^{11},x^{13},x^{18}, and x^{19}. As illustrated in Figure A1 , differentiation and regeneration work generally in this model.

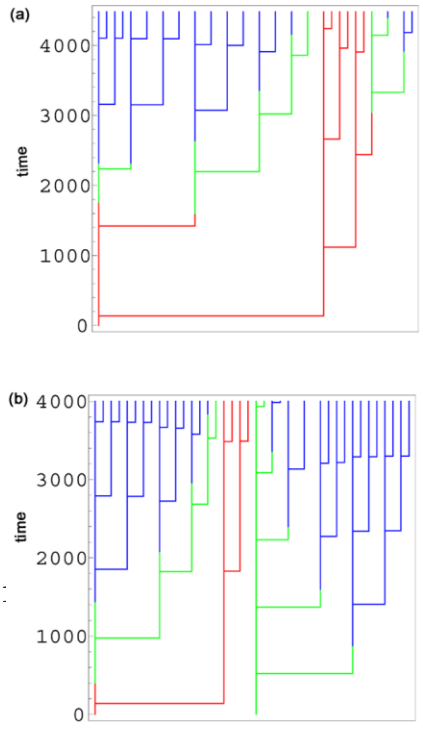

Fig. A1. Regeneration experiment for another network. **a:** The cell-lineage diagram when starting with T_1. **b:** The cell-lineage diagram when starting with T_1T_2. The same segment, $T_3T_2T_1^4T_2T_3$ is regenerated.